Applied Catalysis B: Environmental 182 (2016) 68–73

Contents lists available at ScienceDirect

Applied Catalysis B: Environmental

journal homepage: www.elsevier.com/locate/apcatb

Constructing carbon-nitride-based copolymers via Schiff base chemistry for visible-light photocatalytic hydrogen evolution

Xiangqian Fan, Lingxia Zhang*, Min Wang, Weimin Huang, Yajun Zhou, Mengli Li, Ruolin Cheng, Jianlin Shi**

Shanghai Institute of Ceramics, Chinese Academy of Sciences, 1295 Ding-xi Road, Shanghai 200050, PR China

ARTICLE INFO

Article history:
Received 9 June 2015
Received in revised form 17 August 2015
Accepted 2 September 2015
Available online 7 September 2015

Keywords:
Carbon nitride
Copolymerization
Schiff base chemistry
Photocatalysis
Water splitting

ABSTRACT

The modification of graphitic carbon nitride (g-C_3N_4) for visible-light photocatalytic water splitting is a very hot topic due to the more and more serious energy and environment problems. Here we report a novel, general and cost-effective approach via Schiff base chemistry to construct aromatics-grafted g-C_3N_4-based copolymers. Based on this general strategy, almost all kinds of aromatics can be grafted into carbon nitride networks. As-synthesized copolymers all show remarkably enhanced and stable visible-light photocatalytic hydrogen evolution performance. In addition, the low cost and small optimized adding amounts of these co-monomers adopted here make the present strategy probably the one of most cost-effective copolymerization approach to construct g-C_3N_4-based copolymer photocatalysts.

1. Introduction

Photocatalytic water splitting for hydrogen evolution by utilizing solar energy is a very attractive and challenging subject for scientists. Since the first discovery of the photocatalytic water splitting performance of TiO_2 [1], a large number of semiconductors based on metal oxides [2], metal (oxy) nitrides [3] and metal (oxy) sulfides [4] etc., have been explored as water splitting photocatalysts. Recently, graphitic carbon nitride (g-C_3N_4), which is a metal-free photocatalyst only consisting of carbon and nitrogen [5], has attracted worldwide attention due to its various excellent merits such as visible light response, high photochemical stability and easy-modified textural/electronic structure, etc. [6]. However, the photocatalytic performance of pristine g-C_3N_4 is mediocre. To enhance its photocatalytic activity, many strategies have been developed. Except for the well-established methods such as doping [7], morphological control [8], coupling and sensitization [9], which have been usually used for modifying inorganic photocatalysts, inspired by the nucleophilicity of the precursors for fabricating g-C_3N_4, a new strategy called copolymerization was designed by Wang et al. At first, they chose barbituric acid as the copolymerization monomer [10]. Later, various organic monomers with cyano and amino groups were adopted [11]. Through this copolymerization strategy, a number of aromatic rings can be incorporated into carbon nitride networks, resulting in a broadened range of visible light response and more efficient charge carrier separation, and therefore, better photocatalytic activity. However, those monomers they selected as the copolymerization blocks are usually of high cost because of their complicated preparations. On the other hand, only limited types of aromatics can be incorporated into carbon nitride networks by those previously reported copolymerization strategies. Therefore, more economic and common strategy is highly expected.

Inspired by the Schiff base chemistry, which is often used to extend π conjugated systems of polymers [12], herein, we firstly chose a series of aromatic aldehydes as co-monomers to construct novel g-C_3N_4-based photocatalysts. Taking terephthalaldehyde as an example, a possible graft path is presented in Scheme 1 (here urea is selected as the precursor to synthesize g-C_3N_4 because of urea-derived g-C_3N_4 has the best photocatalytic performance compared with those obtained from other precursors [13]). These terephthalaldehyde modified g-C_3N_4 copolymers were denoted as CNAL-*X*, where *X* (mg) represents the amount of aldehyde added in precursors. The different reaction path between the previous and our copolymerization strategies [10,11] lead to the different structure between the final copolymers. In this work, the aromatic rings

* Corresponding author. Fax: +86 2152413122.
** Corresponding author.
E-mail addresses: zhlingxia@mail.sic.ac.cn (L. Zhang), jlshi@mail.sic.ac.cn (J. Shi).

http://dx.doi.org/10.1016/j.apcatb.2015.09.006
0926-3373/

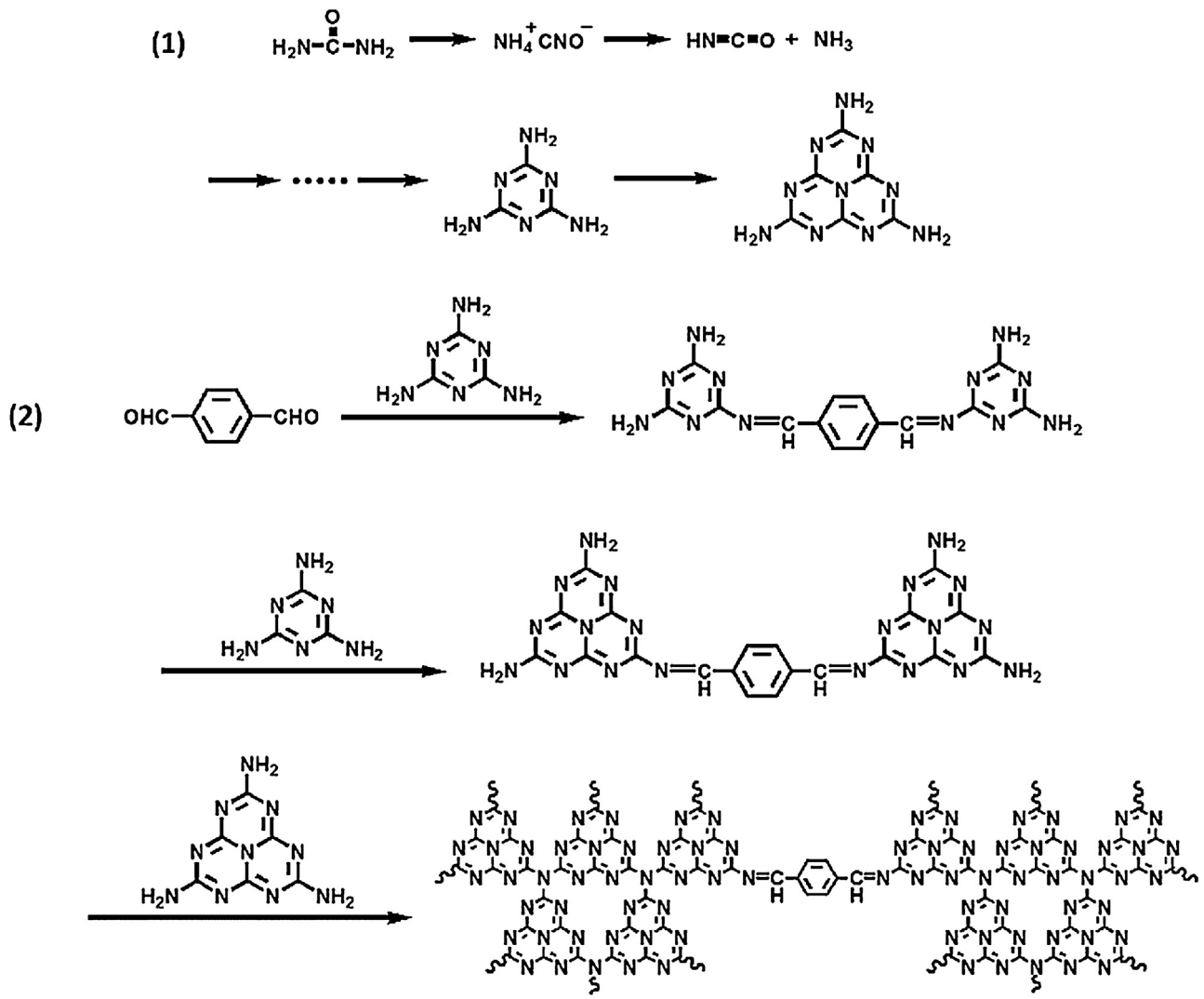

Scheme 1. A possible copolymerization path between terephthalaldehyde and urea at gradually elevated temperature to give CNAL-*X*s.

are connected by adjacent 3,s-triazine units but in the previous report they are incorporated into the inner 3,s-triazine units.

2. Experimental

2.1. Materials

Urea (>99%) was purchased from Sinopharm Chemical Reagent Co., Ltd.; terephthalaldehyde (>98%), 2-naphthaldehyde (>98%), 9-anthracenecarboxaldehyde (>98%), phenanthrene-9-carboxaldehyde (>97%), benzo[b]furan-2-carboxaldehyde (>99%), pyrrole-2-carboxaldehyde (>98%), indole-3-carboxaldehyde (>98%), 2-quinolinecarboxaldehyde (>96%) and 2,6-pyridinedicarboxaldehyde (>98%), 2,5-furandicarboxaldehyde (>98%) and benzo[b]thiophene-3-carboxaldehyde (>98%) were purchased from TCI Co., Ltd.; 2,5-thiophenedicarboxaldehyde (>99%), triethanolamine (>97%) and chloroplatinic acid hexahydrate (>37.5%, Pt basis) were purchased from Sigma–Aldrich Co., LLC.

2.2. Synthetic procedures

In a typical synthesis procedure, 20 g urea and a certain amount of aromatic aldehydes were mixed thoroughly and then the mixture was put in an alumina crucible with a cover and heated to 550 °C for 2 h at a heating rate of 5 °C/min. After undergoing various reactions at high temperature, as-constructed copolymer were obtained.

2.3. Characterization

The X-ray diffraction (XRD) patterns were recorded on a Rigaku-Ultima IV diffractometer. Fourier transform infrared (FT-IR) spectra were obtained with Nicolet iS10 FTIR spectrometer. X-ray photoelectron spectroscopy (XPS) measurements were carried out on a Thermo Scientific ESCALAB 250 spectrometer with Al Kα radiation as the excitation source. Binding energies for the high resolution spectra were calibrated by setting C 1 s to 284.6 eV. High resolution FT-IR spectra were conducted on Nicolet Avatar 330 FTIR spectrometer. Solid-state ^{13}C NMR spectra were performed using a Bruker Advance III 600spectrometer. The transmission electron microscope (TEM) images were obtained on a transmission electron microscope (JEM-1400) and scanning electron microscopy (SEM) images were obtained on a field emission scanning electron microscope (Hitachi SU 82,220). The BET surface areas were measured at a MicromeriticsTristar 3000 system. Elemental analysis (C, H, N) was taken on VARIO EL CUBE microanalyzer. UV–vis diffuse reflectance spectra were performed on a Shimadzu UV-3600 system. Photoluminescence (PL) spectra were recorded at room temperature

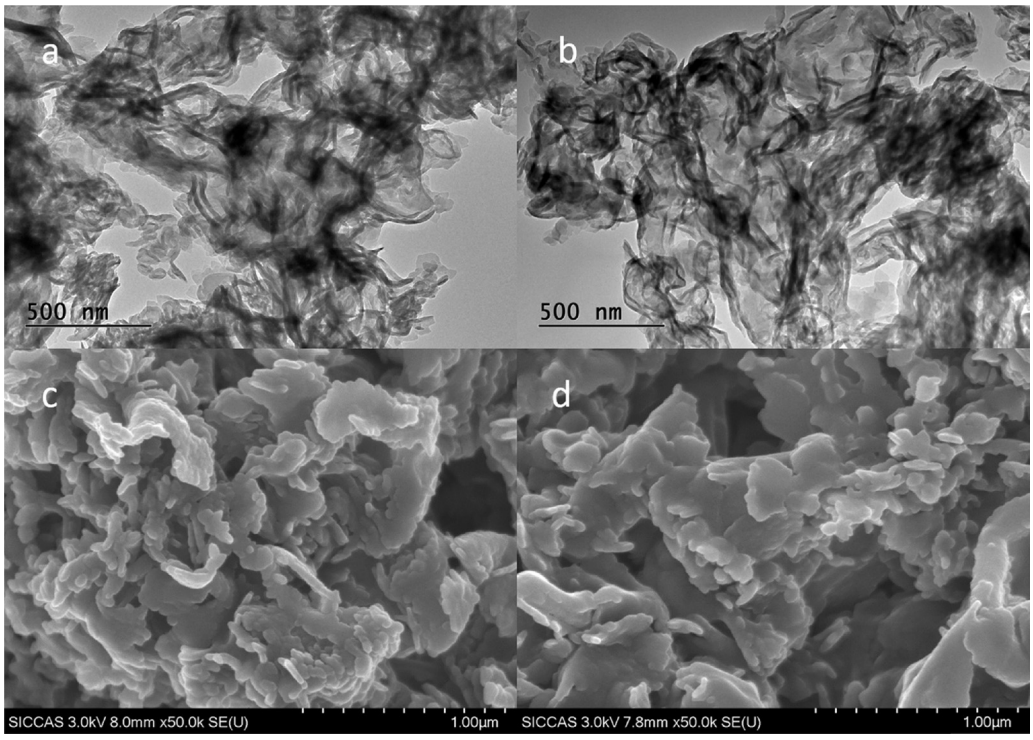

Fig. 1. Typical TEM and SEM images of CN (a and c, respectively) and CNAL-2 (b and d, respectively).

with a fluorescence spectrophotometer (Edinburgh Instruments, FLSP-920). The Excitation wavelength is 380 nm. Electrochemical measurement were conducted with a CHI 760 electrochemical workstation in a conventional three electrode cell, using a Pt plate and an Ag/AgCl electrode as counter electrode and reference electrode, respectively. Working electrodes were obtained by transferring photocatalyst suspensions (10 mg in 3 ml ethanol) onto FTO conductive glass with spin-coating method, the electrodes were annealed at 150° for 2 h. A 0.2 M Na_2SO_4 aqueous solution was chosen as the supporting electrolyte and was purged with nitrogen to remove O_2 before any measurements. The visible light was generated by a 300 W Xe lamp with 420 nm and IR cut-off filters, and was chopped manually.

2.4. Photocatalytic hydrogen evolution test

The photocatalytic reactions were carried out in a quartz reaction vessel connected to a closed gas circulation and evacuation system. 0.1 g catalyst was suspended in 100 ml aqueous solution containing triethanolamine (10 vol%) as the sacrificial electron donor. 3 wt% Pt was loaded on the surface of the carbon nitride catalyst by an in-situ photodeposition method using $H_2PtCl_6{\cdot}6H_2O$ as the precursor. The suspension was thoroughly degassed and irradiated by a 300 W Xe lamp equipped with an optical UV–IR cut-off filter ($780\ nm > \lambda > 420\ nm$) to eliminate UV and IR light. The temperature of the reactant solution was maintained at 283 K by a flow of cooling water during the reaction. The evolved gas was analyzed every 1 h by gas chromatography equipped with a thermal conductive detector. For stability test, the system was evacuated every 4 h and repeated 4 times (i.e., a 16 h recycling experiment with intermittent evacuation every 4 h).

3. Results and discussion

XRD patterns and FT-IR spectra of CN and CNAL-*X*s are presented in Fig. S1. As can be seen, CN and CNAL-*X*s show a similar crystalline structure. All samples exhibit two distinct XRD peaks. The one located at ~12.8° is attributed to in-plane structural repeating motifs. The other one centered at ~27.6° corresponds to the interlayer reflection of the graphitic structure [13][13a]. Both CN and CNAL-*X*s show typical IR patterns of g-C_3N_4. The intense peak at 812 cm^{-1} is assigned to the out-of-plane deformation vibration modes of triazinerings. The several peaks centered at 1200–1600 cm^{-1} are attributed to the stretching vibration modes of 3,s-triazine heterocyclic (C_6N_7) rings. The broad band located at 3000–3500 cm^{-1} is mainly associated with —NH vibration of the uncondensed amino groups [13][13a]. After the incorporation of aromatics in g-C_3N_4 networks, many C—NH groups have been replaced by C═N groups, so the absorption band for CNAL-*X*s has been obviously weakened. In addition, pristine g-C_3N_4 (CN) exhibits an extra absorption peak at ~2349 cm^{-1} belonging to the adsorbed CO_2 molecules [13][13b], while CNAL-*X*s does not. This is because that the grafted aromatic groups result in decreased density of terminal —NH_2 groups, which act as anchors of CO_2 molecules. The XRD patterns and FT-IR spectra of CNAL-*X*s show all the characteristic peaks of CN, demonstrating the main chemical skeleton has been retained. In fact, the morphorlogy of CN has also nearly been unchanged (Fig. 1). In both XRD patterns and IR spectra, CNAL-*X*s show lower intensities than CN, indicating that grafted aromatic groups would interrupt the periodic structure of g-C_3N_4. Because of the enriched C and H elements in phenyl groups, grafting them into carbon nitride networks would increase the C/N ratio and H contents, which can be confirmed by elemental analysis (Table S1). In general, with the increasing amount of phenyl groups grafted, the C/N ratio and H contents will gradually increase. However, because the abundant adsorbed CO_2 molecules in CN contribute much C amount, as demonstrated by the FT-IR spectra, the C/N ratio in CN is higher than that in CNAL-*X* ($1 \le X \le 4$).

To confirm the chemical states of carbon and nitrogen before and after modification, XPS measurements were conducted. Fig. S2 shows the high resolution C1s and N1s XPS spectra of CN and CNAL-2. As can be seen, CNAL-2 shows all the characteristic C and

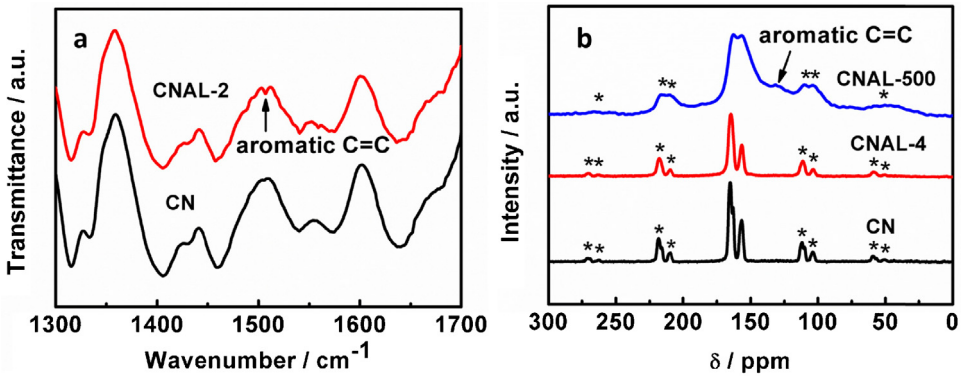

Fig. 2. (a) High-resolution FT-IR spectra of CN and CNAL-2; (b) solid-state ^{13}C NMR spectra of CN, CNAL-4 and CNAL-500. * indicates the spinning side bands in the ^{13}C spectra.

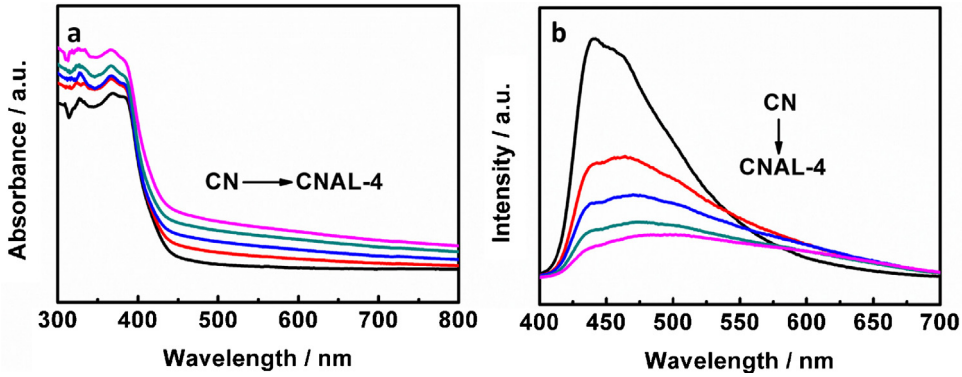

Fig. 3. (a) UV–vis absorption spectra and (b) PL spectra (excitation wavelength = 380 nm) of all the samples obtained.

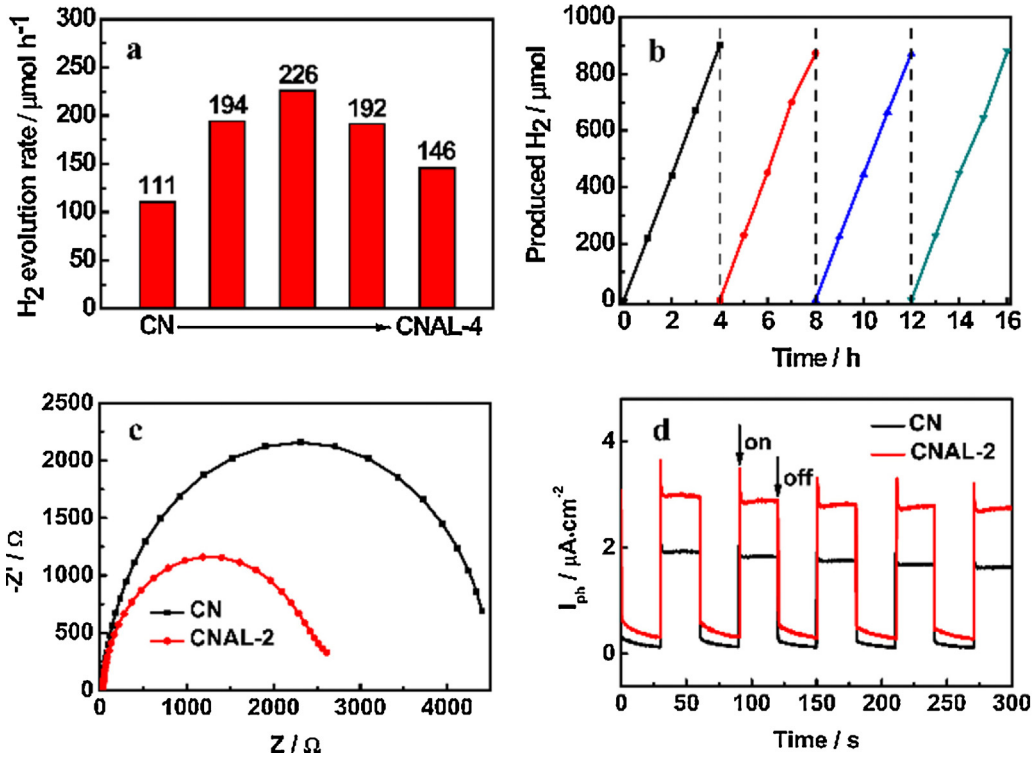

Fig. 4. (a) Hydrogen evolution rates of CN and CNAL-*X*s (*X* = 1–4); (b) cycling stability test of CNAL-2; (c) electrochemical impedance spectroscopy (EIS) Nyquist plots in the dark; (d) Periodic on/off photocurrent responses for CN and CANL-2 under visible-light irradiation.

Representative aromatics		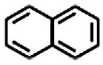	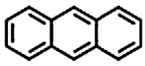	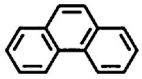
Corresponding precursors	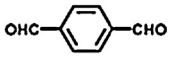	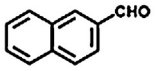	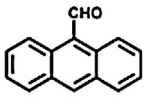	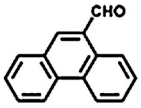
HER (μmol h^{-1})	226	218	255	236
Representative aromatics				
Corresponding precursors	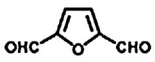	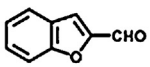	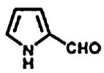	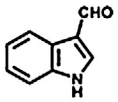
HER (μmol h^{-1})	270	332	280	130
Representative aromatics				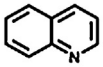
Corresponding precursors	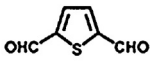	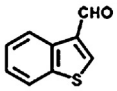	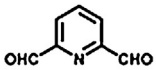	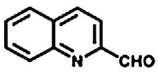
HER (μmol h^{-1})	323	358	343	294

Fig. 5. Representative aromatics that can be grafted into carbon nitride networks and their corresponding precursors. (HER = Hydrogen evolution rate; the dosage of all the precursors is 2 mg).

N peaks of CN. There are no obvious differences but the signal intensity between the spectra of CN and CNAL-2. To further verify whether the aromatic groups have been successfully grafted into carbon nitride networks, CN and CNAL-*X*s were selected to conduct high resolution FT-IR and solid-state ^{13}C NMR measurements. As can be seen in Fig. 2a, CNAL-2 exhibits an extra weak IR band locating at 1506 cm^{-1}, which is attributed to aromatic C=C signals (the band around ~1500 cm^{-1} is known as the strongest band in aromatics). Fig. 2b shows the solid-state ^{13}C NMR spectra of CN, CANL-4 (slightly-modified CN) and CNAL-500 (deeply modified CN). All the samples show the characteristic peaks (156.6 and 165.1 ppm) of 3,s-triazine-based g-C_3N_4. Due to the structure disturbance by aromatics grafting, the resolution of these peaks and the signal to noise ratio of ^{13}C NMR spectra become gradually lower [11][11a]. An additional broad peak centering at 131.7 ppm ascribed to aromatic C=C (usually located at 100–150 ppm) is observed for CNAL-500. CNAL-4 exhibits a similar spectrum with CN because the aromatics in its structure are too few to induce any response by solid-state NMR.

Grafting the aromatics into the carbon nitride networks will undoubtedly alter the electron distribution of the system, and thus alter the intrinsic electronic/optical properties of resultant copolymers, which is demonstrated by the UV–vis absorption spectra of CN and CNAL-*X*s (Fig. 3a). With the increase in the amount of grafted aromatics, a clear red shift of the optical absorption is observed. The PL peaks (Fig. 3b) of the samples also shift to longer wavelength with increasing grafted aromatics. This indicates that grafting aromatics into carbon nitride networks will extend π-conjugation and narrow the band gap of g-C_3N_4 (Fig. S3, Table S2), which is beneficial for absorbing visible-light and thus helpful to elevate the photocatalytic performance. In addition, more and more distinct PL quenching is observed with the increasing grafted aromatics, which is on account of the more distorted structure of CNAL-*X*s (above XRD patterns and FT-IR spectra demonstrate that the structure of CN will be distorted by grafted aromatics). Generally speaking, compared with the rigid planar structure of CN, distorted less rigid structure of CNAL-*X*s is more probable of intramolecular collision, which will result in the energy dissipation of excitons and thus lead to PL quenching.

The photocatalytic hydrogen evolution rates of all the samples are presented in Fig. 4a. Clearly, the copolymers show significantly enhanced photocatalytic hydrogen evolution efficiency over the pure g-C_3N_4. CNAL-2 shows the best photocatalytic performance with a hydrogen evolution rate of 226 μmol h^{-1}. To test its photo-stability, a long time photocatalytic experiment was conducted, as displayed in Fig. 4b, the hydrogen evolution rate shows no noticeable deterioration during 16 h. In addition, the XRD pattern and FT-IR spectra (Fig. S4) also show no obvious variation, proving its high photo-stability. The copolymerization of aromatics with carbon nitride frameworks would stop the polymerization of heptazine units, and thus create pores at their docking sites. This is another advantage to tune the texture of carbon nitride, as in the case of increasing its specific surface area, by copolymerization (Table S2). The enlarged BET surface area should make some contributions to the improved photocatalytic activity of these copolymers. Besides, it is known that the photo-reduction

ability of semiconductor is determined by the potential of its conduction band (LUMO), higher LUMO position means stronger photo-reduction ability. By conducting the valence band X-ray photoelectron spectroscopy measurements [14], the HOMO of CN and CNAL-2 were estimated to be 2.08 eV and 1.93 eV (Fig. S5), respectively. Therefore, the corresponding LUMO of CN and CNAL-2 were calculated to be −0.85 eV and −0.98 eV, respectively, from the formula $Eg = E_{HOMO} - E_{LUMO}$. The higher LUMO of CNAL-2 over CN would endow it with stronger photo-reduction ability (Fig. S6). In Fig. 4c, an obvious decrease in semicircular Nyquist plots is observed for CNAL-2, demonstrating that incorporating aromatics into carbon nitride networks can effectively improve the electronic conductivity of the polymer matrix. The enlarged photocurrent generated on CNAL-2 over CN (Fig. 4d) further confirms the higher separation and transfer efficiency of its photogenerated carriers [10,11,13,14][10,11,13b,14], which is also a key factor deciding its photocatalytic performance. With more aromatics being grafted, the structure of g-C_3N_4 would become more disordered/distorted, consequently more energy of photo-generated charge carriers will dissipate into forms of vibrational/thermal energy, etc., resulting in gradually decreased photocatalytic activity.

In principle, through this strategy, almost all sorts of aromatics can be grafted into carbon nitride networks by adding these aromatics-related aldehyde (mono-aldehyde or multi-aldehyde) into the precursors of g-C_3N_4. Fig. 5 gives the hydrogen evolution rates of some representative aromatics-grafted g-C_3N_4. As-synthesized copolymers all show much enhanced photocatalytic hydrogen evolution activity. By selecting appropriate aromatic co-monomers, more efficient photocatalysts based on g-C_3N_4 can be expected. Fig. S7 shows the hydrogen evolution rates on 2,6-pyridinedicarboxaldehyde modified and 2,5-thiophenedicarbox-aldehyde modified g-C_3N_4, combined with Fig. 4a, we can see the optimized adding amount of the monomers is as low as ~2–3 mg/g carbon nitride (20 urea generates ~0.9 g carbon nitride), while those well-established copolymerization methods reported before [10,11] need ~20–50 mg co-monomers per gram carbon nitride to reach their optimized hydrogen evolution performance. The extra low dosage of monomer precursors, along with their relatively cheaper price, suggests this copolymerization strategy is much more economic and competitive in practical utilizations.

4. Conclusions

A new copolymerization strategy based on Schiff base chemistry has been presented to fabricate novel aromatics-grafted carbon nitrides. The structural and electronic properties of carbon nitride can be easily modified by small amounts of co-monomers added. As-obtained copolymers show substantially enhanced photocatalytic hydrogen evolution efficiency over pristine carbon nitride. Through this facile strategy, almost all kinds of aromatics can be grafted into carbon nitride networks, paving a way to exploring more efficient g-C_3N_4-based photocatalysts. In addition, the low cost and small optimized adding amounts of these co-monomers adopted here make the present strategy probably the one of most cost-effective copolymerization approach to construct carbon-nitride-based copolymer photocatalysts.

Acknowledgements

The authors gratefully acknowledge financial support from National Key Basic Research Program of China (2013CB933200), National 863 plans projects (2012AA062703), National Natural Science Foundation of China (Grant No. 21177137), and Youth Innovation Promotion Association CAS (2012200).

Appendix A. Supplementary data

Supplementary data associated with this article can be found, in the online version, at http://dx.doi.org/10.1016/j.apcatb.2015.09.006.

References

[1] A. Fujishima, K. Honda, Nature 238 (1972) 37.
[2] (a) R. Asahi, T. Morikawa, T. Ohwaki, K. Aoki, Y. Taga, Science 293 (2001) 269;
(b) Z. Zou, J. Ye, K. Sayama, H. Arakawa, Nature 414 (2001) 625;
(c) H.G. Kim, D.W. Hwang, J.S. Lee, J. Am. Chem. Soc. 126 (2004) 8912.
[3] (a) K. Maeda, K. Teramura, D. Lu, T. Takata, N. Saito, Y. Inoue, K. Domen, Nature 440 (2006) 295;
(b) K. Maeda, T. Takata, M. Hara, N. Saito, Y. Inoue, H. Kobayashi, K. Domen, J. Am. Chem. Soc. 127 (2005) 8286;
(c) W. Luo, Z. Li, X. Jiang, T. Yu, L. Liu, X. Chen, J. Ye, Z. Zou, Phys. Chem. Chem. Phys. 10 (2008) 6717.
[4] (a) N. Kakuta, K.H. Park, M.F. Finlayson, A. Ueno, A.J. Bard, A. Campion, M.A. Fox, S.E. Webber, J.M. White, J. Phys. Chem. 89 (1985) 732;
(b) I. Tsuji, H. Kato, H. Kobayashi, A. Kudo, J. Am. Chem. Soc. 126 (2004) 13406;
(c) I. Tsuji, Y. Shimodaira, H. Kato, H. Kobayashi, A. Kudo, Chem. Mater. 22 (2010) 1402.
[5] X. Wang, K. Maeda, A. Thomas, K. Takanabe, G. Xin, J.M. Carlsson, K. Domen, M. Antonietti, Nat. Mater. 8 (2009) 76.
[6] (a) Y. Wang, X. Wang, M. Antonietti, Angew. Chem. Int. Ed. 51 (2012) 68;
(b) Y. Zheng, J. Liu, J. Liang, M. Jaroniec, S.Z. Qiao, Energy Environ. Sci. 5 (2012) 6717;
(c) Z. Zhao, Y. Sun, F. Dong, Nanoscale 7 (2014) 15;
(d) X. Wang, S. Blechert, M. Antonietti, ACS Catal. 2 (2012) 1596.
[7] (a) J. Li, B. Shen, Z. Hong, B. Lin, B. Gao, Y. Chen, Chem. Commun. 48 (2012) 12017;
(b) Z. Ding, X. Chen, M. Antonietti, X. Wang, ChemSusChem 4 (2011) 274;
(c) G. Zhang, M. Zhang, X. Ye, X. Qiu, S. Lin, X. Wang, Adv. Mater. 26 (2014) 805;
(d) X. Chen, J. Zhang, X. Fu, M. Antonietti, X. Wang, J. Am. Chem. Soc. 131 (2009) 11658;
(e) Y. Wang, Y. Di, M. Antonietti, H. Li, X. Chen, X. Wang, Chem. Mater. 22 (2010) 5119;
(f) G. Dong, K. Zhao, L. Zhang, Chem. Commun. 48 (2012) 6178;
(g) Y. Zhang, T. Mori, J. Ye, M. Antonietti, J. Am. Chem. Soc. 132 (2010) 6294.
[8] (a) J. Xu, Y. Wang, Y. Zhu, Langmuir 29 (2013) 10566;
(b) X. Wang, K. Maeda, X. Chen, K. Takanabe, K. Domen, Y. Hou, X. Fu, M. Antonietti, J. Am. Chem. Soc. 131 (2009) 1680;
(c) J. Sun, J. Zhang, M. Zhang, M. Antonietti, X. Fu, X. Wang, Nat. Commun. (2012) 1139;
(d) S. Yang, Y. Gong, J. Zhang, L. Zhan, L. Ma, Z. Fang, R. Vajtai, X. Wang, P.M. Ajayan, Adv. Mater. 25 (2013) 2452;
(e) P. Niu, L. Zhang, G. Liu, H.-M. Cheng, Adv. Funct. Mater. 22 (2012) 4763.
[9] (a) J. Zhang, M. Zhang, R.Q. Sun, X. Wang, Angew. Chem. Int. Ed. 51 (2012) 10145;
(b) Y.-P. Yuan, S.-W. Cao, Y.-S. Liao, L.-S. Yin, C. Xue, Appl. Catal. B-Environ. 140–141 (2013) 164;
(c) H. Yan, Y. Huang, Chem. Commun. 47 (2011) 4168;
(d) M. Bledowski, L. Wang, A. Ramakrishnan, O.V. Khavryuchenko, V.D. Khavryuchenko, P.C. Ricci, J. Strunk, T. Cremer, C. Kolbeck, R. Beranek, Phys. Chem. Chem. Phys. 13 (2011) 21511;
(e) Y. Hou, A.B. Laursen, J. Zhang, G. Zhang, Y. Zhu, X. Wang, S. Dahl, I. Chorkendorff, Angew. Chem. Int. Ed. 52 (2013) 3621.
[10] J. Zhang, X. Chen, K. Takanabe, K. Maeda, K. Domen, J.D. Epping, X. Fu, M. Antonietti, X. Wang, Angew. Chem. Int. Ed. 49 (2010) 441.
[11] (a) J. Zhang, G. Zhang, X. Chen, S. Lin, L. Mohlmann, G. Dolega, G. Lipner, M. Antonietti, S. Blechert, X. Wang, Angew. Chem. Int. Ed. 51 (2012) 3183;
(b) G. Zhang, X. Wang, J. Catal. 307 (2013) 246;
(c) J. Zhang, M. Zhang, S. Lin, X. Fu, X. Wang, J. Catal. 310 (2014) 24;
(d) M. Zhang, X. Wang, Energy Environ. Sci. 7 (2014) 1902.
[12] (a) F. Tsai, C. Chang, C. Liu, W. Chen, S. Jenekhe, Macromolecules 38 (2005) 1958;
(b) S. Barik, T. Bletzacker, W. Skene, Macromolecules 45 (2012) 1165;
(c) H. Deng, B. Zhu, L. Song, C. Tu, F. Qiu, Y. Shi, D. Wang, L. Zhu, X. Zhua, Polym. Chem. 3 (2012) 421.
[13] (a) J. Liu, T. Zhang, Z. Wang, G. Dawson, W. Chen, J. Mater. Chem. 21 (2011) 14398;
(b) G. Zhang, J. Zhang, M. Zhang, X. Wang, J. Mater. Chem. 22 (2012) 8083.
[14] (a) G. Liu, L. Wang, C. Sun, X. Yan, X. Wang, Z. Chen, S. Smith, H. Cheng, G. Lu, Chem. Mater. 21 (2009) 1266;
(b) G. Liu, P. Niu, L. Yin, H.-M. Cheng, J. Am. Chem. Soc. 134 (2012) 9070.